

Cite this: *Dalton Trans.*, 2018, **47**, 15091

## Synthesis, cytotoxic activity and DNA interaction studies of new dinuclear platinum(II) complexes with an aromatic 1,5-naphthyridine bridging ligand: DNA binding mode of polynuclear platinum(II) complexes in relation to the complex structure†

Bata Konovalov,<sup>a</sup> Marija D. Živković,<sup>b</sup> Jelena Z. Milovanović,<sup>c</sup> Dragana B. Djordjević,<sup>c</sup> Aleksandar N. Arsenijević,<sup>c</sup> Ivana R. Vasić,<sup>b</sup> Goran V. Janjić,<sup>d</sup> Andjela Franich,<sup>a</sup> Dragan Manojlović,<sup>e,f</sup> Sandra Skrivanj,<sup>e</sup> Marija Z. Milovanović,<sup>c</sup> Miloš I. Djuran<sup>g</sup> and Snežana Rajković<sup>h</sup>  <sup>h</sup>\*

The synthesis, spectroscopic characterization, cytotoxic activity and DNA binding evaluation of seven new dinuclear platinum(II) complexes **Pt1–Pt7**, with the general formula  $[\{Pt(L)Cl\}_2(\mu\text{-}1,5\text{-nphe})](ClO_4)_2$  (1,5-nphe is 1,5-naphthyridine; while L is two amines (**Pt1**) or one bidentate coordinated diamine: ethylenediamine (**Pt2**), ( $\pm$ )-1,2-propylenediamine (**Pt3**), *trans*-( $\pm$ )-1,2-diaminocyclohexane (**Pt4**), 1,3-propylenediamine (**Pt5**), 2,2-dimethyl-1,3-propylenediamine (**Pt6**), and 1,3-pentanediamine (**Pt7**)), were reported. *In vitro* cytotoxic activity of these complexes was evaluated against three tumor cell lines, murine colon carcinoma (CT26), murine mammary carcinoma (4T1) and murine lung cancer (LLC1) and two normal cell lines, murine mesenchymal stem cells (MSC) and human fibroblast (MRC-5) cells. The results of the MTT assay indicate that all investigated complexes have almost no cytotoxic effects on 4T1 and very low cytotoxicity toward LLC1 cell lines. In contrast to the effects on LLC1 and 4T1 cells, complexes **Pt1** and **Pt2** had significant cytotoxic activity toward CT26 cells. Complex **Pt1** had a much lower  $IC_{50}$  value for activity on CT26 cells compared with cisplatin. In comparison with cisplatin, all dinuclear **Pt1–Pt7** complexes showed lower cytotoxicity toward normal MSC and MRC-5 cells. In order to measure the amount of platinum(II) complexes taken up by the cells, we quantified the cellular platinum content using inductively coupled plasma mass spectrometry (ICP-QMS). Molecular docking studies performed to evaluate the potential binding mode of dinuclear platinum(II) complexes **Pt1–Pt7** and their aqua derivatives **W1–W7**, respectively, at the double stranded DNA showed that groove spanning and backbone tracking are the most stable binding modes.

Received 14th May 2018,  
Accepted 18th September 2018  
DOI: 10.1039/c8dt01946k

rsc.li/dalton

<sup>a</sup>University of Kragujevac, Faculty of Science, Department of Chemistry, R. Domanovića 12, 34000 Kragujevac, Serbia. E-mail: snezana@kg.ac.rs

<sup>b</sup>University of Kragujevac, Faculty of Medical Sciences, Department of Pharmacy, Svetozara Markovića 69, 34000 Kragujevac, Serbia

<sup>c</sup>University of Kragujevac, Faculty of Medical Sciences, Department of Microbiology and immunology, Center for Molecular Medicine and Stem Cell Research, Svetozara Markovića 69, 34000 Kragujevac, Serbia

<sup>d</sup>University of Belgrade, Institute of Chemistry, Technology and Metallurgy, Njegoševa 12, 11000 Belgrade, Serbia

<sup>e</sup>University of Belgrade, Faculty of Chemistry, Studentski trg 12-16, 11000 Belgrade, Serbia

<sup>f</sup>South Ural State University, Lenin prospekt 76, 454080 Chelyabinsk, Russia

<sup>g</sup>Serbian Academy of Sciences and Arts, Knez Mihailova 35, 11000 Belgrade, Serbia

† Electronic supplementary information (ESI) available: Tables S1–S3, Fig. S1–S14 and Schemes S1 and S2. See DOI: 10.1039/c8dt01946k

## Introduction

Platinum-based drugs as classical chemotherapeutic agents have been widely applied in treating solid tumors, especially cisplatin, which is considered as the fundamental component of standard chemotherapy.<sup>1–3</sup> The anticancer activity of cisplatin is based on its ability to form intrastrand covalent adducts with DNA by binding of Pt to the N7 atoms of two adjacent guanine bases.<sup>4,5</sup> The negative side effects during treatment (such as nephrotoxicity, ototoxicity, cardiotoxicity, neurotoxicity, vomiting, resistance, *etc.*) encouraged researchers to design new classes of platinum complexes with improved anti-tumor properties.<sup>6,7</sup> Polynuclear platinum complexes represent a novel class of promising antitumor agents with potential clinical significance.<sup>8</sup> These complexes have more than one

platinum centers which are linked through a flexible bridge such as an aliphatic chain,<sup>6</sup> or a rigid bridge that consists, for instance, of azole molecules.<sup>7</sup> Some of the azole-bridged dinuclear platinum(II) complexes are highly effective *in vitro* in cisplatin-resistant cell lines, as well as in several tumor cell lines.<sup>9,10</sup> The development of research in this area was driven by the hypothesis that complexes with distinctly different DNA-binding mechanisms may exhibit unique biological activity in comparison with current mononuclear clinically used agents.<sup>11</sup>

DNA molecules play a key role in controlling cellular functions, and hence is considered an excellent drug target, most notably for cancer. Reactive ligands form covalent bonds with DNA (intrastrand and interstrand cross-links, Fig. S1†), although in most cases the drugs form non-covalent association through electrostatic, hydrogen-bonding and  $\pi$ - $\pi$  stacking interactions (groove binding and intercalation, Fig. S2†).<sup>12,13</sup> The main binding modes for small molecules are intercalation and minor-groove binding. The bindings into the minor groove have a significantly higher DNA sequence selectivity and efficiency,<sup>12–14</sup> while the intercalation is followed by conformational changes of DNA, due to the formation of a binding cavity,<sup>12,13</sup> which is not required for minor-groove binding. The majority of intercalating drugs have a preference to GC-rich regions,<sup>14,15</sup> while the drugs bonded into the minor groove show preferences to binding to AT-rich regions.<sup>13,16,17</sup> The proteins often occupy the major groove, and the biological activity of these proteins is often determined by minor-groove binding drugs.<sup>14</sup>

Highly-charged polynuclear platinum(II) complexes are a class of antitumor agents with wide capacity and new manner of DNA binding (backbone tracking or groove spanning, Fig. S3†),<sup>18</sup> structurally distinct from those formed by the metal complexes and by other organic compounds (Fig. S1 and S2†). Recently, another class of dinuclear platinum(II) complexes with six-membered heterocyclic diazines as the bridging ligands,  $[\{Pt(L)Cl\}_2(\mu\text{-pz})]^{2+}$  (L is ethylenediamine (en), ( $\pm$ )-1,2-propylenediamine (1,2-pn), *trans*-( $\pm$ )-1,2-diaminocyclohexane (dach), 1,3-propylenediamine (1,3-pd), 2,2-dimethyl-1,3-propylenediamine (2,2-diMe-1,3-pd), ( $\pm$ )-1,3-pentanediamine (1,3-pnd) and pz is the pyrazine bridging ligand),<sup>19–21</sup> as well as  $[\{Pt(en)Cl\}_2(\mu\text{-pydz})]^{2+}$  (pydz is the bridging pyridazine ligand),<sup>22</sup> have been synthesized and were developed and evaluated in bioassays for further potential development towards novel anticancer agents. The cytotoxic potential of these dinuclear Pt(II) complexes in comparison with cisplatin was tested on human lung fibroblasts (MRC5) and two carcinoma cell lines, melanoma (A375) and colon cancer (HCT116) by the MTT assay.<sup>23</sup> It was found that  $[\{Pt(1,3\text{-pd})Cl\}_2(\mu\text{-pz})]^{2+}$  showed improved and  $[\{Pt(en)Cl\}_2(\mu\text{-pydz})]^{2+}$  showed comparable activity to that of clinically relevant cisplatin.<sup>23</sup> As a continuation of our ongoing interest towards the chemistry of platinum(II) with bridging nitrogen-containing heterocyclic ligands,<sup>23</sup> in the light of the fact that polynuclear Pt(II) complexes represent promising antitumor

agents, in the present paper we report the synthesis and spectroscopic characterization of seven new  $[\{Pt(L)Cl\}_2(\mu\text{-1,5-nphe})]^{2+}$  complexes (**Pt1–Pt7**), all differing in the ligand L (L is two amines ( $\text{NH}_3$ ) **Pt1** or bidentate coordinated diamines: ethylenediamine (en) **Pt2**, ( $\pm$ )-1,2-propylenediamine (1,2-pn) **Pt3**, *trans*-( $\pm$ )-1,2-diaminocyclohexane (dach) **Pt4**, 1,3-propylenediamine (1,3-pd) **Pt5**, 2,2-dimethyl-1,3-propylenediamine (2,2-diMe-1,3-pd) **Pt6**, and 1,3-pentanediamine (1,3-pnd) **Pt7**, and 1,5-nphe is the bridging 1,5-naphthyridine ligand) (Fig. 1). *In vitro* cytotoxic activity of the **Pt1–Pt7** complexes was evaluated against three tumor cell lines, murine colon carcinoma (CT26), murine mammary carcinoma (4T1) and murine lung cancer (LLC1), and two normal cell lines, murine mesenchymal stem cells (MSC) and human fibroblast (MRC-5) cells. The uptake of the platinum(II) complexes into the cells was investigated. The cytotoxicity and cellular uptake of all these complexes were compared with those of cisplatin. The binding studies of these complexes with calf thymus DNA (CT-DNA) were studied by UV-vis absorption and fluorescence spectroscopy. A molecular docking study is performed to evaluate the potential binding mode of the dinuclear platinum(II) complexes **Pt1–Pt7** and their aqua derivatives **W1–W7**, respectively, at double stranded DNA.

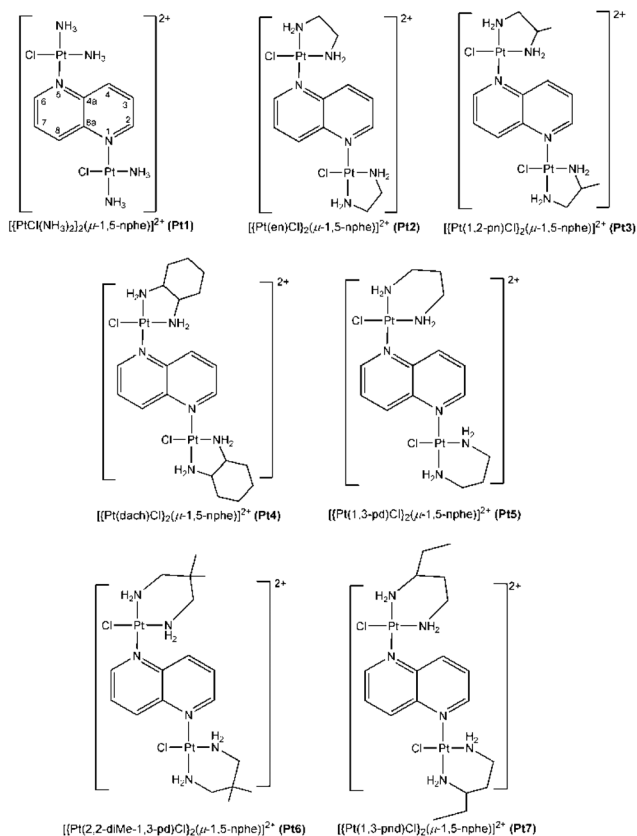


**Fig. 1** Schematic drawing of the  $[\{Pt(L)Cl\}_2(\mu\text{-1,5-nphe})]^{2+}$  complexes **Pt1–Pt7** (L is  $2\text{NH}_3$  or a bidentate coordinated diamine ligand: en, 1,2-pn, dach, 1,3-pd, 2,2-diMe-1,3-pd and 1,3-pnd; 1,5-nphe is 1,5-naphthyridine).

## Results and discussion

### Synthesis and spectroscopic characterization of dinuclear Pt(II) complexes Pt1–Pt7

Seven new 1,5-naphthyridine-bridged (1,5-nphe) dinuclear platinum(II) complexes **Pt1–Pt7**, with the general formula  $[\{Pt(L)Cl\}_2(\mu\text{-}1,5\text{-nphe})](ClO_4)_2$ , have been synthesized and characterized by elemental microanalysis, NMR ( $^1H$  and  $^{13}C$ ), IR and UV-vis spectroscopy (Fig. 1; L is two amines ( $NH_3$ ) **Pt1**, or bidentate coordinated diamine: ethylenediamine (en) **Pt2**, ( $\pm$ )-1,2-propylenediamine (1,2-pn) **Pt3**, *trans*-( $\pm$ )-1,2-diaminocyclohexane (dach) **Pt4**, 1,3-propylenediamine (1,3-pd) **Pt5**, 2,2-dimethyl-1,3-propylenediamine (2,2-diMe-1,3-pd) **Pt6**, and ( $\pm$ )-1,3-pentanediamine (1,3-pnd) **Pt7**).

Our attempts to crystallize these complexes from their amorphous powders using different solvents (water, methanol, acetone, chloroform, and dimethylformamide) were unsuccessful. As can be seen from Fig. 1, all these complexes have the same 1,5-naphthyridine-bridged ligand, but differ in the nature of the ligand L. Thus, complex **Pt1** contains two amine ( $NH_3$ ) ligands while in the other six complexes **Pt2–Pt7** these two amines are replaced with different bidentate coordinated diamine ligands. In comparison with complexes **Pt2–Pt4**, all having a five-membered ethylenediamine ring, complexes **Pt5–Pt7** contain a six-membered 1,3-propanediamine ring. The schematic presentation of the reaction for the synthesis of complexes **Pt1–Pt7** is given in Scheme S1.† The corresponding mononuclear  $[Pt(L)Cl_2]$  complex was reacted with an equimolar amount of  $AgNO_3$  in DMF solution to replace one chloride ligand with a DMF molecule. To the monoactivated  $[Pt(L)Cl(DMF)]^+$  species 1,5-naphthyridine (1:0.5 molar ratio, respectively) was added and resulting mixture was stirred at room temperature to form the 1,5-naphthyridine-bridged dinuclear Pt(II) complex. The obtained solution was evaporated to dryness, and complexes **Pt1–Pt7** were obtained as perchlorate salts from water solution in an excess of  $LiClO_4$ .

**Spectroscopic characterization.** The proton chemical shifts for the free 1,5-nphe ligand and investigated dinuclear platinum(II) complexes **Pt1–Pt7** in  $D_2O$  are reported in Table S1.† In the aromatic region, the  $^1H$  NMR spectra of complexes **Pt1–Pt7** consist of three sets of resonances attributed to the protons of the Pt(II)-coordinated 1,5-nphe ligand (C2H and C6H, C4H and C8H, and C3H and C7H), with the chemical shifts differing from those of the uncoordinated 1,5-nphe ligand. As can be seen from Table S1,† these resonances for the complexes **Pt1–Pt7** are shifted downfield in comparison with those for the free bridging ligand. The downfield shifting of the protons in the 1,5-nphe ligand after its platination can be ascribed to a delocalization of the charge deficiency (cation formation by Pt(II) coordination) throughout all of the rings in the molecule as anticipated.<sup>24,25</sup> Considering all aromatic protons, the significant values of the  $\Delta(^1H)_{coord}$  coordination shifts are +0.68 and +1.81 ppm for all complexes **Pt1–Pt7**.

It is important to note that the  $^1H$  chemical shifts for the aliphatic methyl, methylene and methine protons of the biden-

tate coordinated ligand L in complexes **Pt1–Pt7** are in agreement with those for the structurally similar dinuclear platinum(II) complexes previously reported.<sup>19–21</sup>

The  $^{13}C$  NMR spectra of **Pt1–Pt7** in  $D_2O$  due to the aromatic carbons display four distinct signals and are noticeably different from those of the uncoordinated 1,5-nphe ligand. Addition of the free 1,5-nphe to the  $D_2O$  solution of the complexes results in the appearance of another set of  $^{13}C$  signals (Table S1†). As a consequence of the Pt(II) complexation of the investigated 1,5-naphthyridine ligand, signals of all the ring carbons are shifted downfield after the bidentate coordination of two equivalent mononuclear platinum(II) units. The chemical shifts of the methyl, methylene and methine carbons of the bidentate coordinated diamine ligand L in **Pt2–Pt7** are identical to those for these carbons of the mononuclear  $[Pt(L)Cl_2]$  complex which are used as the starting material for the preparation of the corresponding dinuclear Pt(II) complexes **Pt1–Pt7**.<sup>19–21</sup>

The UV-vis absorption spectra of **Pt1–Pt7** in water at a concentration of  $5 \times 10^{-5}$  M are shown in Fig. S4.† The wavelengths of maximum absorption for these complexes ( $\lambda_{max}$ , nm) and the molar extinction coefficients ( $\epsilon$ ,  $M^{-1} cm^{-1}$ ) determined right after the dissolution of the complexes are listed in the Experimental section. Similar spectral shapes and values of the  $\lambda_{max}$  were obtained for all the complexes suggesting the same coordination mode of 1,5-naphthyridine. The absorption maxima within a wavelength range of  $\sim 316\text{--}317$  nm have been observed for all the complexes and attributed to the LMCT (ligand-to-metal charge transfer) transition. The observed bathochromic shift of the absorbance peak can be attributed to the  $\pi \rightarrow \pi^*$  transitions in the 1,5-naphthyridine ligand after its coordination to the Pt(II) ion.

The IR spectral data of **Pt1–Pt7** complexes are listed in the Experimental section. The IR spectra of the complexes recorded in the wave number range of  $4000\text{--}450$   $cm^{-1}$  show the bands attributable to the vibration of the coordinated N-heterocyclic aromatic ligand (1,5-nphe), as well as those due to the bidentate coordinated diamine ligands and perchlorate counter anion. In addition, the complexes **Pt1–Pt7** display two very strong and sharp bands, which are attributed to the asymmetric ( $\sim 3300$   $cm^{-1}$ ) and symmetric ( $3200$   $cm^{-1}$ ) stretching vibrations of the coordinated amino group of diamine ligands.<sup>26</sup> The IR spectra of all **Pt1–Pt7** complexes show a very strong band with two sub-maxima at  $1174\text{--}1080$   $cm^{-1}$  and a strong one at  $\sim 625$   $cm^{-1}$  which can be distinguished and ascribed to the  $\nu(ClO)$  and  $\delta(OClO)$  modes, respectively, of the uncoordinated perchlorates.<sup>27</sup>

### Cytotoxic activity and uptake assays of the platinum(II) complexes

The results of the MTT assay indicate that all seven newly synthesized dinuclear Pt(II) complexes **Pt1–Pt7** have almost no cytotoxic effect on murine mammary carcinoma cell lines, 4T1 and very low cytotoxicity toward murine lung cancer cells, LLC1 (Fig. S5†). In both cases complex **Pt1** exerted the highest cytotoxic potential, especially toward LLC1 cells. The percen-

**Table 1** IC<sub>50</sub> (mM) for the 72 h of action of the Pt(II) complexes and cisplatin on 4T1, CT26, LLC1, MSC and MRC-5 cells, as determined by the MTT assay. The data are presented as the mean values ± SD (standard deviation) from three experiments

Complex	Cell lines				
	4T1	CT26	LLC1	MSC	MRC-5
<b>Pt1</b>	64.5 ± 9.2	3.3 ± 1.0	18.2 ± 3.1	8.1 ± 1.3	37.0 ± 1.7
<b>Pt2</b>	191.3 ± 36.2	42.0 ± 7.2	111.7 ± 16.3	121.8 ± 3.1	378.7 ± 4.0
<b>Pt3</b>	523.6 ± 83.6	>1000	337.7 ± 56.2	117.6 ± 2.5	310.8 ± 4.9
<b>Pt4</b>	193.2 ± 39.5	174.9 ± 18.9	119.7 ± 20.0	66.8 ± 3.8	93.8 ± 11.4
<b>Pt5</b>	327.2 ± 76.1	>1000	183.8 ± 21.4	133.5 ± 6.9	198.2 ± 2.5
<b>Pt6</b>	185.7 ± 22.0	331.0 ± 92.1	171.4 ± 22.1	120.0 ± 8.2	150.6 ± 3.3
<b>Pt7</b>	186.2 ± 31.5	483.5 ± 87.6	159.9 ± 18.5	72.2 ± 12.8	135.2 ± 3.9
<b>Cisplatin</b>	<7.8	29.1 ± 5.9	<7.8	<7.8	<7.8

tage of viable LLC1 cells after exposure to complex **Pt1** and cisplatin at a concentration of 62.5 μM was similar (Fig. S5†). With respect to cisplatin, all dinuclear platinum(II) complexes showed lower cytotoxic effects on the two normal cells, murine mesenchymal stem cells (MSC) and human fibroblasts (MRC-5). Analysis of IC<sub>50</sub> values also indicates very low cytotoxic activity of the investigated platinum(II) complexes on 4T1 and LLC1 cells (Table 1). Complex **Pt1** had the highest activity toward murine colon carcinoma LLC1 (IC<sub>50</sub> is 18.2 ± 3.1) and 4T1 (IC<sub>50</sub> is 64.5 ± 9.2) cells, but still much weaker compared with the activity of cisplatin (IC<sub>50</sub> < 7.8). In contrast to the effects on LLC1 and 4T1 cells, complexes **Pt1** and **Pt2** had significant cytotoxic activity toward CT26 murine colon carcinoma cells. Although complex **Pt2**, at the lowest tested concentrations, had better cytotoxic activity toward murine colon carcinoma cells (CT26) in comparison with cisplatin, the IC<sub>50</sub> value for complex **Pt2** was higher than the IC<sub>50</sub> for cisplatin (Table 1). However, complex **Pt1** had a much lower IC<sub>50</sub> value for activity on CT26 cells compared with cisplatin (Table 1). Complexes **Pt1** and **Pt2** showed selective activity toward the tumor cell line CT26 in comparison with murine MSC and MRC-5 (Table 1). The IC<sub>50</sub> value of **Pt1** for CT26 cells was 2.5 and 12 times lower in comparison with those for MSC and MRC-5, respectively. Nearly, the same difference between the IC<sub>50</sub> values for CT26, MSC and MRC-5 was found for complex **Pt2** (Table 1).

For the determination of the potential for the induction of apoptotic death of the tested **Pt1–Pt7** complexes flow cytometry analysis of CT26 cells stained with Annexin V and PI after exposure to these complexes (concentration 15 μM) for 24 hours was done. Our results indicate that all tested complexes after 24 hours induce the apoptotic death of CT26 cells (Fig. 2). According to the MTT viability assay, complexes **Pt1** and **Pt2** had higher cytotoxic effects on CT26 compared to cisplatin (concentration 15 mM), based on the detection of Annexin V stained cells.

There are two known pathways by which Pt-based anti-cancer agents most likely enter the cell: passive diffusion through the plasma membrane and active transport by a number of transport proteins.<sup>28</sup> The active transport of platinum complexes includes, Cu transporters (Ctrs), organic cation transporters (OCTs), solute carriers (SLCs) and ATP-

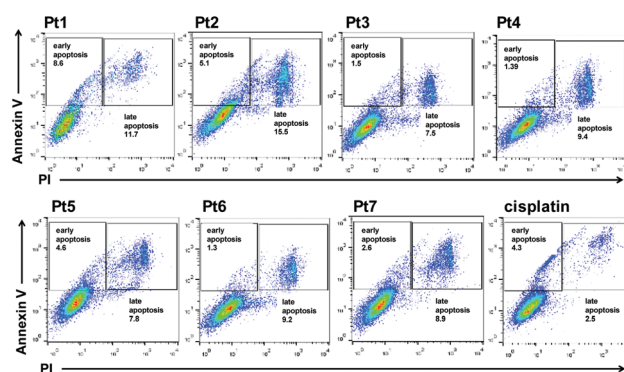


**Fig. 2** Representative flow plots showing the percentages of early apoptotic, late apoptotic and viable CT26 cells after 24 h of treatment with the platinum(II) complexes (concentration: 15 mM).

binding cassette (ABC) multidrug transporters.<sup>28</sup> In order to measure the amount of dinuclear **Pt1–Pt7** complexes and cisplatin taken up by tumor cells, we quantified the cellular platinum content in LLC1 cells using inductively coupled plasma mass spectrometry (ICP-QMS). The results of six independent experiments are depicted in Fig. 3 and Table S2.† All investigated dinuclear Pt(II) complexes showed a higher level of cellular uptake compared to cisplatin. Complex **Pt1** which contains two Pt(II) units structurally similar to cisplatin along with **Pt2**

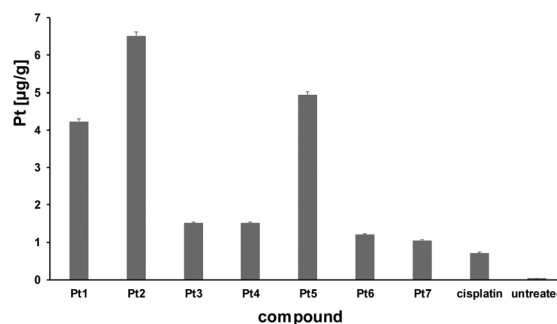


**Fig. 3** Cell uptake of **Pt1–Pt7** complexes and cisplatin by LLC1 cells after 2 h of treatment at 37 °C with compounds at 2 μM in DMSO. The data are shown as the mean values ± standard deviations from six independent experiments.

and **Pt5** complexes, both containing the five-membered ethylenediamine and six-membered 1,3-propanediamine rings, respectively, display significantly higher levels (5–9 times) of the cellular uptake in comparison to those for the other presently investigated dinuclear complexes. The low cellular uptake of **Pt3**, **Pt4**, **Pt6** and **Pt7** complexes results from the fact that ethylenediamine (**Pt3** and **Pt4**) and 1,3-propanediamine (**Pt6** and **Pt7**) rings have an alkyl substituent which has an impact on the uptake of the Pt(II) complex into the cell. As there is no drastic difference in the size of **Pt2** and **Pt3** complexes (ethylenediamine derivatives), and between **Pt5**, **Pt6** and **Pt7** complexes (1,3-propanediamine derivatives), it is obvious that the passive transport is not responsible for the differences in the cellular uptake level of the investigated dinuclear Pt(II) complexes. Namely, the introduction of alkyl substituents increases the electron density on chelate rings and the hydrophobic area of the complex, but also decreases the flexibility of the rings. The flexibility of unsubstituted five- and six-membered rings is due to the rapid ring inversion (ring flipping). A ring flipping of the substituted diamine rings to the conformation with the axial (or pseudoaxial) substituent is unfavourable because of the steric repulsion between the substituents occupying the axial (or pseudoaxial) positions.<sup>29</sup> It is known that molecular recognition is driven primarily by enthalpic effects, determined by the formation of specific interactions between the protein and the ligand, while the entropic effect, reflected through the ligand flexibility, could compensate the weaker interactions of these two species.<sup>30</sup> In our case, the greater flexibility of unsubstituted chelate diamine rings allows a better accessibility of NH<sub>2</sub> groups for hydrogen bonding, as well as a greater conformational freedom of the complexes in contact with biomolecules. This is probably the reason why the **Pt1**, **Pt2** and **Pt5** complexes are bound to a loop of human serum transferrin, while the remaining complexes are bound in the area between the two helices (results of the docking study are shown in Fig. S6 and S7†). In addition, the remaining complexes (**Pt3**, **Pt4**, **Pt6** and **Pt7**) are bound close to Met313, confirmed by NMR as the coordination binding center of Pt compounds at the N-lobe of the transferrin. The main function of transferrin is the binding and transport of metal ions (primarily iron ions) into the cell *via* receptor-mediated endocytosis, and the results of the docking study have shown that small amounts of **Pt3**, **Pt4**, **Pt6** and **Pt7** complexes are coordinated to transferrin, that affect the amount of complexes entering the cell. On the other hand, the results of the docking study also point to the similarities in the binding of these complexes to protein, and it can be considered as a reason for the similar cellular uptake.

### Interaction of the platinum(II) complexes with DNA

**Spectroscopic studies.** The interaction of dinuclear **Pt1–Pt7** complexes with calf thymus DNA (CT-DNA) has been monitored by UV-vis spectroscopy in aqueous phosphate buffer solution (PBS) at pH 7.40 and 37 °C. The absorption spectra of dinuclear **Pt2** and **Pt5** complexes in the absence and in the presence of increasing amounts of CT-DNA at a constant con-

centration of the Pt(II) complex are shown in Fig. S8.† The obtained results for the other presently investigated dinuclear Pt(II) complexes are almost identical to those presented in Fig. S8.† As is shown in this figure, the absorption intensity of the dinuclear **Pt2** and **Pt5** complexes decreased slightly after the addition of CT-DNA (H% ≈ 5, hypochromism). However, no change in the absorption wavelength maximum at 317 nm was observed in the presence of increasing amounts of CT-DNA. These observations could be attributed to the presence of electrostatic interactions between the positively charged platinum(II) complexes and the negatively charged DNA backbone, which is in accordance with the results obtained from the molecular docking study performed for the hydrolyzed **Pt1–Pt7** complexes (renamed as **W1–W7**, respectively) and double stranded DNA.

The binding of dinuclear **Pt1–Pt7** complexes to CT-DNA was also studied by the fluorescence technique. The emission spectra of the CT-DNA-EtBr system in the absence and in the presence of increasing amounts of the platinum(II) complexes were measured in 0.01 M in PBS at pH 7.40 and room temperature. The obtained results presented in Fig. S9† for **Pt2** and **Pt5** complexes, respectively, show that the fluorescence intensity of the CT-DNA-EtBr system decreases slightly after the addition of the platinum(II) complex, which indicates very weak binding of the investigated platinum(II) complexes to DNA.

**Molecular docking study.** Molecular docking is a useful technique for the prediction of the drug binding mode to DNA (Fig. S1–S3†), although nucleic acids are more flexible than proteins.<sup>31–34</sup> In this work, the molecular docking study was performed to evaluate the potential binding mode of dinuclear  $[\{Pt(L)(H_2O)\}_2(\mu-1,5-nphe)]^{4+}$  complexes (**W1–W7**; Fig. 4) which represent aqua derivatives of the corresponding chloride platinum(II) complexes **Pt1–Pt7**, respectively.

Binding energies of the most stable adducts are in the range from –8.60 to –10.63 kcal mol<sup>–1</sup>, (Table 2). In the adducts illustrated in Fig. 4, the hydrogen bonds between the

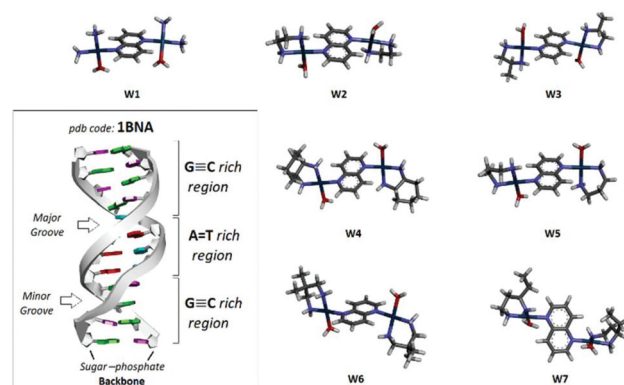


**Fig. 4** The structures of DNA (pdb code-1BNA) and optimized structures of dinuclear  $[\{Pt(L)(H_2O)\}_2(\mu-1,5-nphe)]^{4+}$  complexes (**W1–W7**) which represent the aqua derivatives of the corresponding chloride platinum(II) complexes **Pt1–Pt7**, respectively.

**Table 2** Summary of the binding energies (in kcal mol<sup>-1</sup>) and results of energy decomposition analysis, for dinuclear platinum(II)-aqua complexes **W1–W7** and DNA, as assessed by molecular docking

Model system	Total energy ( $E_t$ )	Decomposition of energy ( $E_t = E1 + E2 + E3 + E4 - E5$ )				
		$E1$	$E2$	$E3$	$E4$	$E5$
<b>W1</b>	-8.60	-2.44	-8.35	+0.59	+2.20	+0.59
<b>W2</b>	-10.63	-2.52	-9.21	+10.63	+1.10	+10.63
<b>W3</b>	-9.14	-2.55	-7.70	+2.29	+1.10	+2.29
<b>W4</b>	-9.33	-3.28	-7.15	+2.22	+1.10	+2.22
<b>W5</b>	-9.38	-3.46	-7.03	+2.45	+1.10	+2.45
<b>W6</b>	-10.27	-3.91	-7.46	+2.74	+1.10	+2.74
<b>W7</b>	-9.47	-4.77	-6.35	+2.35	+1.65	+2.35

$E_t$  - Estimated free energy of binding.  $E1$  - vdW + Hbond + desolv energy.  $E2$  - Electrostatic energy.  $E3$  - Final total internal energy.  $E4$  - Torsional free energy.  $E5$  - Unbound system's energy.

(Pt)-N-H and (Pt)-O-H groups of the metal complex and backbone oxygens of DNA (Fig. S10–S13<sup>†</sup>) result in either the groove spanning or backbone tracking binding mode. The difference in the binding energies is a result of the different number of hydrogen bonds, their geometry as well as whether the (Pt)-O-H or (Pt)-N-H groups are involved in hydrogen bonding. However, the results of energy decomposition analysis (Table 2) show that the electrostatic energy ( $E2$ ) has a greater contribution in attraction than the energy of hydrogen bonding ( $E1$ ). Namely, there is very strong coulombic attraction between the positively charged metal complexes (+4) and the negatively charged DNA backbone. These findings are in agreement with the results of UV-vis spectroscopy, that are attributed to the presence of electrostatic interactions between the positively charged platinum(II) complexes and the negatively charged DNA backbone.

The docking study was also performed for the chloride Pt(II) complexes **Pt1–Pt7**, and the results showed that groove spanning is the most stable binding mode in the majority of the structures (Fig. S14<sup>†</sup>), except for the complexes **Pt3** and **Pt6**, where the minor groove bonding occurs in the most stable orientation, in the G-C rich region of DNA. The groove spanning binding mode is strongly favoured, despite the fact that **Pt1–Pt7** complexes are less charged (+2), compared to the corresponding Pt(II) aqua complexes (+4) (Fig. 5).

#### DNA binding mode of polynuclear platinum(II) complexes in relation to the complex structure

It is known that the polynuclear platinum(II) complexes (PPCs) could be divided into the class of complexes that form covalent bonds with DNA (such as triplatin tetranitrate, Scheme S2,<sup>†</sup> the only “non-classical” platinum-based cytotoxic drug to enter clinical trials for the treatment of human cancer) and the class of non-covalently binding complexes, mainly with substitutionally inert PtN<sub>4</sub> coordination spheres.<sup>35</sup> The crystal structure of the DNA adduct with the non-covalently bonded trinuclear platinum(II) complex (triplatinNC, Scheme S2<sup>†</sup>)

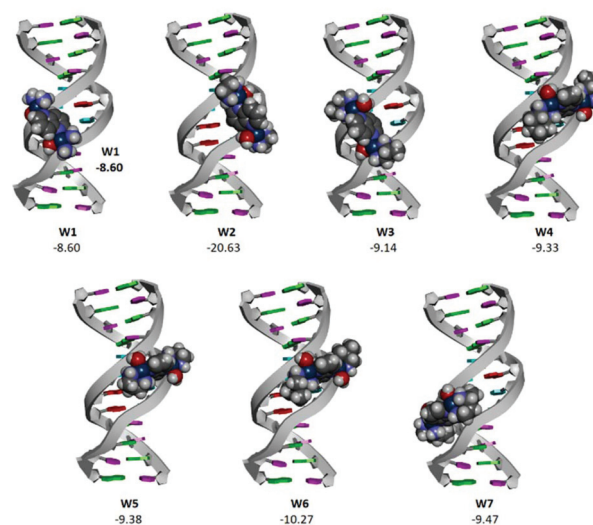


**Fig. 5** The structures of the most stable binding modes of dinuclear platinum(II) complexes **W1–W7** to DNA, as assessed by molecular docking. These complexes represent the aqua derivatives of the corresponding chloride platinum(II) complexes **Pt1–Pt7**, respectively.

showed a new binding motif, slightly different from that of the conventional intercalation and groove binding mode, which is called a phosphate clamp motif, including the backbone tracking and groove-spanning modes.<sup>36</sup> The presently reported results demonstrate this unique phosphate clamp binding motif of +2 charged complexes, non-covalently bonded to DNA, also through the groove spanning and backbone tracking binding modes. Five dinuclear Pt(II) complexes, **Pt1**, **Pt2**, **Pt4**, **Pt5** and **Pt7**, prefer groove spanning as a binding mode, while the minor groove bonding is found to be the most stable binding mode for only two complexes, **Pt3** and **Pt6**. The results of the docking study on the hydrolysed complexes **W1–W7** (aqua derivatives of the corresponding chloride **Pt1–Pt7** complexes, respectively) have shown that these complexes have the tendency to the groove spanning binding mode (except the **W7** complex which has a slightly greater tendency to the backbone tracking binding mode). In our complexes, the replacement of the central tetraammine unit of triplatin derivatives by 1,5-naphthyridine did not lead to changes in the binding motif of the complexes, except that the considered dinuclear Pt(II) complexes show slightly more affinity towards the groove spanning binding mode.

It is also known that the polynuclear platinum(II) complexes of biologically important polyamines, spermidine and spermine show a superficial resemblance to triplatin derivatives (Scheme S2<sup>†</sup>). The incorporation of linear polyamines into the triplatin polynuclear framework produces a class of polynuclear complexes that replicate the biological activity of triplatin derivatives,<sup>37,38</sup> but with different binding profiles. Namely, the spermidine and spermine complexes prefer the formation of long-range inter-strand crosslinks.<sup>39</sup>

Earlier studies of dinuclear Pt(II) complexes, with coordinated polyamines and with the general formula

$[\{\text{Pt}(\text{NH}_3)_3\}_2(\mu\text{-(H}_2\text{N(CH}_2)_n\text{NH}_2))\}]^{4+}$ , showed that metal complexes are significantly more effective initiators of conformational transitions of suitable DNA structures (B  $\rightarrow$  Z and B  $\rightarrow$  A conformations), compared to uncoordinated spermine.<sup>40,41</sup> The groove spanning binding mode displays a slightly greater influence on the tertiary structure of superhelical and B-DNA, that strongly suggest the condensation of DNA.<sup>42</sup> As a consequence of this, there is a displacement of intercalated ethidium bromide (EtBr) from the DNA double helix to the solution, accompanied by a quenching of its fluorescence, and a cooperative facilitation of minor-groove binding.<sup>42</sup> The cooperative binding was explained as a result of the minor groove expansion caused by phosphate clamps of a polynuclear platinum(II) complex,<sup>35,36,43</sup> while the quenching of EtBr fluorescence was connected to condensation effects (conformational changes on the tertiary structure of DNA) that disfavour the intercalation of EtBr. It is also known that triplatinNC and triplatinNC-A are significantly more effective condensing agents compared to uncoordinated spermine.<sup>44,45</sup> The quenching of the EtBr fluorescence and groove spanning binding mode, predicted by the docking study indicates that the binding of our considered platinum (II) complexes leads to condensation of DNA.

The triplatinNC-type complexes display a slight preference to the backbone tracking mode in the G–C rich region of DNA, while the groove-spanning binding displays slight affinity for the A–T rich region,<sup>42,45,46</sup> The results of the docking studies have shown that our dinuclear Pt(II) complexes have a higher affinity to groove spanning binding, that actually occurred in the A–T rich region, while the less common binding (backbone tracking) is shifted toward the G–C rich region. Differences in the preferred binding modes between our complexes and the triplatinNC-type complexes are caused by the differences in the nature of bridging ligands. Our complexes have a very rigid bridging ligand, with an aromatic character (1,5-naphthyridine), while the central unit of triplatinNC-type-derivatives is a tetraammine fragment, with a pronounced tendency to electrostatic interactions and hydrogen bonding. Although our complexes satisfy the structural requirements for the crosslinking of DNA (contains two Pt–Cl coordination bonds), it is obvious that the bridging ligand has a decisive role for preference to the groove spanning binding mode.

Three factors with the greatest impact on the cytotoxicity of the Pt complexes are cellular uptake, metabolic transformation of the complexes through the reaction with biomolecules, as well as the formation of adducts with DNA. Increasing the positive charge of the polynuclear Pt(II) complex leads to an increase in the cellular uptake, hence the cellular uptake of TriplatinNC is significantly enhanced over that of the “parent” Triplatin.<sup>47</sup> The noncovalent binding of TriplatinNC in comparison with the coordinative binding of cisplatin is the reason for the very high cellular uptake. Our results are in line with this observation, because all tested dinuclear complexes showed a slightly higher cellular uptake compared to cisplatin. Replacement of the chloride ligand of Triplatin by  $-\text{NH}_3$  or the

amine ligand (as in the case of TriplatinNC-A and TriplatinNC) prevents metabolic deactivation. For this reason, the treatment of A2780 ovarian carcinoma cells with HSA-bound TriplatinNC (TriplatinNC/HSA) showed identical cytotoxicity, cellular accumulation, and DNA adduct formation compared to the treatment with TriplatinNC alone.<sup>48</sup> In contrast, the HSA-bound cisplatin and Triplatin (cisplatin/HSA and Triplatin/HSA), showed dramatic decreases of cytotoxic profiles and the levels of cellular accumulation.<sup>48</sup> An *in vivo* study showed that TriplatinNC does not covalently bind to serum proteins, due to its high charge and the absence of a substitution-labile leaving group, that would allow the complex to undergo the same types of deactivation reactions as seen with the coordinatively bound platinum analogues.<sup>49</sup> However, TriplatinNC demonstrated cytotoxic activity in a wide range of human tumor cell lines, at micromolar concentrations, like cisplatin.<sup>47</sup> The biological action of TriplatinNC-A and TriplatinNC may be associated with the unique ability of these complexes to induce the nucleic acid condensation and aggregation of small transfer RNA molecules, and consequently to the inhibition effects on topoisomerase-I mediated relaxation of supercoiled DNA.<sup>50</sup> Despite the similar binding modes of our complexes to DNA, compared to TriplatinNC, the differences in their cytotoxicity can be attributed to a smaller positive charge of our complexes (+2) and the presence of chemically active Pt–Cl bonds, that make our complexes slightly different chemical agents for the reaction with biomolecules.

## Conclusions

In this paper, the synthesis, spectroscopic characterization, and cytotoxic and DNA binding evaluation of seven new dinuclear Pt(II) complexes **Pt1–Pt7**, with the general formula  $[\{\text{Pt}(\text{L})\text{Cl}\}_2(\mu\text{-1,5-nphe})](\text{ClO}_4)_2$  (L is two amines **Pt1** or different bidentate coordinated diamines: en, **Pt2**; 1,2-pn, **Pt3**; dach, **Pt4**; 1,3-pd, **Pt5**; 2,2-diMe-1,3-pd, **Pt6**; 1,3-pnd, **Pt7** and 1,5-nphe is 1,5-naphthyridine as a bridging ligand) were reported. *In vitro* cytotoxic activity of the complexes was evaluated against three tumor cell lines, murine colon carcinoma (CT26), murine mammary carcinoma (4T1) and murine lung cancer (LLC1) and two normal cell lines, murine mesenchymal stem cells (MSC) and human fibroblast (MRC-5) cells. The results of the MTT assay indicate that all investigated complexes have almost no cytotoxic effects on 4T1 and very low cytotoxicity toward LLC1 cell lines. Complexes **Pt1** and **Pt2** have significant cytotoxic activity toward CT26 cells, comparable with cisplatin. The molecular docking study, performed for the chloride Pt(II) complexes and their aqua derivatives, showed that groove spanning is the most stable DNA binding mode in the majority of the investigated complexes. This study reveals the DNA binding modes of dinuclear Pt(II) complexes containing an aromatic 1,5-naphthyridine bridging ligand and helps in further insight into the structure–function paradigm of platinum(II) antitumor compounds.

## Experimental

### Materials and methods

Distilled water was demineralized and purified to a resistance greater than  $10 \text{ M}\Omega \text{ cm}^{-1}$ . The compounds deuterium oxide ( $\text{D}_2\text{O}$ ), ethylenediamine (en), ( $\pm$ )-1,2-propylenediamine (1,2-pn), *trans*-( $\pm$ )-1,2-diaminocyclohexane (dach), 1,3-propylenediamine (1,3-pd), 2,2-dimethyl-1,3-propylenediamine (2,2-diMe-1,3-pd), ( $\pm$ )-1,3-pentanediamine (1,3-pnd), 1,5-naphthyridine (1,5-nphe), ethidium bromide (EtBr), calf thymus DNA (CT-DNA) and  $\text{K}_2[\text{PtCl}_4]$  were obtained from Sigma-Aldrich Chemical Co. A stock solution of CT-DNA was prepared in 0.01 M phosphate buffered saline (PBS) buffer (Sigma Aldrich) at pH = 7.4, which gave a ratio of UV absorbance at 260 nm and 280 nm (A260/A280) of *ca.* 1.8–1.9, indicating that DNA was sufficiently free of protein contamination. The concentration of DNA was determined by UV absorbance at 260 nm ( $\epsilon = 6600 \text{ M}^{-1} \text{ cm}^{-1}$ ).<sup>51,52</sup> Elemental microanalyses for carbon, hydrogen and nitrogen were performed by the Microanalytical Laboratory, Faculty of Chemistry, University of Belgrade. All pH measurements were made at room temperature. The pH meter (S220 SevenCompact, pH/Ion, Mettler Toledo) was calibrated with a buffer solution of pH 4.00 and 7.00. The UV-vis spectra were recorded on a Shimadzu double-beam spectrophotometer equipped with thermostatted 1.00 cm quartz Suprasil cells, after dissolving the corresponding dinuclear platinum(II) complexes in water, over the wavelength range of 200–600 nm. The concentration of the dinuclear Pt(II) complexes was  $5 \times 10^{-5} \text{ M}$ . The infrared spectra were recorded as KBr pellets on a PerkinElmer Spectrum One spectrometer over the range 4000–450  $\text{cm}^{-1}$ . The  $^1\text{H}$  and  $^{13}\text{C}$  NMR spectra were recorded on a Varian Gemini 2000 spectrometer ( $^1\text{H}$  at 200 MHz,  $^{13}\text{C}$  at 50 MHz) using 5 mm NMR tubes, at 25 °C in  $\text{D}_2\text{O}$  containing TSP (sodium 3-(trimethylsilyl)propionate) as the internal reference. The chemical shifts are reported in parts per million (ppm) and scalar couplings are reported in hertz (Hz). The NMR samples were prepared in  $\text{D}_2\text{O}$  as the solvent and the total volume was 0.6 mL. Fluorescence measurements were carried out on a RF-1501 PC spectrofluorometer (Shimadzu, Japan). The excitation and emission bandwidths were both 10 nm. The HRMS spectra were measured on an Agilent 6224 Accurate Mass TOF LC/MS instrument at the University of Ljubljana.

### Synthesis of dinuclear platinum(II) complexes Pt1–Pt7

Dinuclear platinum(II) complexes **Pt1–Pt7** were prepared from the corresponding mononuclear  $[\text{Pt}(\text{L})\text{Cl}_2]$  complexes (L is  $2\text{NH}_3$  (**Pt1**), en (**Pt2**), 1,2-pn (**Pt3**), dach (**Pt4**), 1,3-pd (**Pt5**), 2,2-diMe-1,3-pd (**Pt6**), and 1,3-pnd (**Pt7**)) by modification of the procedure published in the literature.<sup>19,20,22,53</sup> The procedure for the preparation of *cis*- $[\text{PtCl}_2(\text{NH}_3)_2]$  was described elsewhere.<sup>54</sup> However, for the preparation of the other mononuclear  $[\text{Pt}(\text{L})\text{Cl}_2]$  complexes we used the method which was slightly modified in accordance with that previously described in the literature.<sup>55–57</sup> To the solution of 207.56 mg (0.50 mmol) of  $\text{K}_2[\text{PtCl}_4]$  dissolved in 10 mL of water was added 332.02 mg

(2.00 mmol) of potassium iodide and the mixture was heated at 50 °C for 5 min. Subsequently, an equimolar amount (0.5 mmol) of the diamine ligand (L) was added to the obtained reaction mixture with heating (50 °C) and stirring continued for 30 min. All  $[\text{Pt}(\text{L})\text{I}_2]$  complexes were crystallized from water at room temperature. The corresponding aqua derivatives of the  $[\text{Pt}(\text{L})\text{I}_2]$  complexes were obtained by treatment with 1.98 equivalents of  $\text{AgNO}_3$  according to a previously published method.<sup>58</sup> The mixture was stirred overnight at room temperature in the dark. In each case, the precipitated  $\text{AgCl}$  was removed by filtration, and in the obtained fresh solutions of the aqua complexes an excess of potassium chloride was added. The pale-yellow precipitate of the  $[\text{Pt}(\text{L})\text{Cl}_2]$  complexes was removed by filtration, washed with methanol and then ether, and air-dried. The yield was between 80–90%. The experimental results of the elemental analysis for C, H and N parameters for all mononuclear Pt(II) complexes are in accordance with the theoretical values calculated for  $[\text{Pt}(\text{L})\text{Cl}_2]$  type complexes.

The mononuclear  $[\text{Pt}(\text{L})\text{Cl}_2]$  complexes were converted into the corresponding monodimethylformamide (DMF) complexes  $[\text{Pt}(\text{L})\text{Cl}(\text{DMF})]^+$  by treatment with 0.98 equivalents of  $\text{AgNO}_3$ . A suspension of  $[\text{Pt}(\text{L})\text{Cl}_2]$  (0.30 mmol) in 10 mL of DMF was added to a solution of  $\text{AgNO}_3$  (49.26 mg, 0.29 mmol) in 5 mL of DMF. The mixture was stirred overnight at room temperature in the dark. The precipitated  $\text{AgCl}$  was removed by filtration and the resulting pale yellow DMF solution of  $[\text{Pt}(\text{L})\text{Cl}(\text{DMF})]^+$  was used for further synthesis of the required 1,5-naphthyridine-bridged platinum(II) complexes.

The DMF solution of 1,5-naphthyridine (10.00 mg, 0.15 mmol) was added dropwise to the solution of  $[\text{Pt}(\text{L})\text{Cl}(\text{DMF})]^+$ . The mixture was stirred at room temperature in the dark for 24 h. After the evaporation of the solvent the residue was washed with ether. The crude product was dissolved in a minimal amount of 0.5 M  $\text{LiClO}_4$  aqueous solution. The obtained solution was left overnight in the dark. The pale-yellow precipitate of the dinuclear Pt(II) complex was removed by filtration, washed with methanol and then ether, and air-dried. Yield was between 35–40%. The purity of the complexes was checked by elemental microanalysis, NMR ( $^1\text{H}$  and  $^{13}\text{C}$ ), UV-vis and IR spectroscopy.

Anal. calcd for **Pt1** ( $\text{C}_8\text{H}_{18}\text{N}_6\text{Cl}_4\text{O}_8\text{Pt}_2$ ; FW = 858.23): C, 11.20%; H, 2.11%; N, 9.79%. Found: C, 11.13%; H, 2.19%; N, 9.65%.  $^1\text{H}$  NMR (200 MHz,  $\text{D}_2\text{O}$ ,  $\delta$ , ppm): 8.24 (dd, 2H, C3H, C7H), 9.69 (d, 2H, C4H, C8H), 10.38 (d, 2H, C2H, C6H).  $^{13}\text{C}$  NMR (50 MHz,  $\text{D}_2\text{O}$ ,  $\delta$ , ppm): 130.5 (C3, C7), 147.4 (C4, C8), 147.5 (C4a, C8a), 161.4 (C2, C6). IR (KBr,  $\nu$ ,  $\text{cm}^{-1}$ ): ~3299, 3225 (N–H stretch); 1622, 1514 (C=N/C=N 1,5-naphthyridine group stretch); 1093, 1083, 625 (perchlorate counter ion). UV-vis ( $\text{H}_2\text{O}$ ,  $\lambda_{\text{max}}$ , nm): 317 ( $\epsilon = 10.5 \times 10^3 \text{ M}^{-1} \text{ cm}^{-1}$ ). ESI-HRMS ( $\text{CH}_3\text{CN}$ ):  $[[\text{PtCl}(\text{NH}_3)_2]_2(\mu-1,5\text{-nphe})\text{ClO}_4]^+$  ( $m/z = 758.97$ ),  $[\text{PtCl}(\text{NH}_3)_2(\mu-1,5\text{-nphe})]^+$  ( $m/z = 395.04$ ),  $[\text{PtCl}(\text{NH}_3)_2]_2(\mu-1,5\text{-nphe})^{2+}$  ( $m/z = 328.51$ ),  $[\text{PtCl}(\text{NH}_3)_2]^+$  ( $m/z = 262.98$ ).

Anal. calcd for **Pt2** ( $\text{C}_{12}\text{H}_{22}\text{N}_6\text{Cl}_4\text{O}_8\text{Pt}_2$ ; FW = 910.31): C, 15.83%; H, 2.44%; N, 9.23%. Found: C, 15.48%; H, 2.56%; N, 8.99%.  $^1\text{H}$  NMR (200 MHz,  $\text{D}_2\text{O}$ ,  $\delta$ , ppm): 8.17 (m, 2H, C3H,

C7H), 9.61 (d, 2H, C4H, C8H), 10.25 (d, 2H, C2H, C6H).  $^{13}\text{C}$  NMR (50 MHz,  $\text{D}_2\text{O}$ ,  $\delta$ , ppm): 129.0 (C3, C7), 141.4 (C4, C8), 147.6 (C4a, C8a), 159.6 (C2, C6). IR (KBr,  $\nu$ ,  $\text{cm}^{-1}$ ):  $\sim$ 3280–3197 (N–H stretch); 1631, 1586, 1511 (C=N/C=N 1,5-naphthyridine group stretch); 1145, 1089, 626 (perchlorate counter ion). UV-vis ( $\text{H}_2\text{O}$ ,  $\lambda_{\text{max}}$ , nm): 317 ( $\epsilon = 11.0 \times 10^3 \text{ M}^{-1} \text{ cm}^{-1}$ ). ESI-HRMS ( $\text{CH}_3\text{CN}$ ):  $[[\{\text{Pt}(\text{en})\text{Cl}\}_2(\mu\text{-1,5-nphe})]\text{ClO}_4]^+$  ( $m/z = 811.00$ ),  $[\text{Pt}(\text{en})\text{Cl}(\mu\text{-1,5-nphe})]^+$  ( $m/z = 421.05$ ),  $[\{\text{Pt}(\text{en})\text{Cl}\}_2(\mu\text{-1,5-nphe})]^{2+}$  ( $m/z = 354.03$ ),  $[\text{Pt}(\text{en})\text{Cl}]^+$  ( $m/z = 290.00$ ).

Anal. calcd for **Pt3** ( $\text{C}_{14}\text{H}_{26}\text{N}_6\text{Cl}_4\text{O}_8\text{Pt}_2$ ; FW = 938.36): C, 17.92%; H, 2.79%; N, 8.96%. Found: C, 17.73%; H, 2.66%; N, 8.89%.  $^1\text{H}$  NMR (200 MHz,  $\text{D}_2\text{O}$ ,  $\delta$ , ppm): 8.16 (d, 2H, C3H, C7H), 9.58 (m, 2H, C4H, C8H), 10.22 (d, 2H, C2H, C6H).  $^{13}\text{C}$  NMR (50 MHz,  $\text{D}_2\text{O}$ ,  $\delta$ , ppm): 130.3 (C3, C7), 142.9 (C4, C8), 147.5 (C4a, C8a), 161.0 (C2, C6). IR (KBr,  $\nu$ ,  $\text{cm}^{-1}$ ):  $\sim$ 235, 3144, 3068 (N–H stretch); 1590, 1514 (C=N/C=N 1,5-naphthyridine group stretch); 1105, 1087, 626 (perchlorate counter ion). UV-vis ( $\text{H}_2\text{O}$ ,  $\lambda_{\text{max}}$ , nm): 317 ( $\epsilon = 9.7 \times 10^3 \text{ M}^{-1} \text{ cm}^{-1}$ ). ESI-HRMS ( $\text{CH}_3\text{CN}$ ):  $[[\{\text{Pt}(1,2\text{-pn})\text{Cl}\}_2(\mu\text{-1,5-nphe})]\text{ClO}_4]^+$  ( $m/z = 839.03$ ),  $[\text{Pt}(1,2\text{-pn})\text{Cl}(\mu\text{-1,5-nphe})]^+$  ( $m/z = 435.07$ ),  $[\{\text{Pt}(1,2\text{-pn})\text{Cl}\}_2(\mu\text{-1,5-nphe})]^{2+}$  ( $m/z = 370.04$ ),  $[\text{Pt}(1,2\text{-pn})\text{Cl}]^+$  ( $m/z = 303.02$ ).

Anal. calcd for **Pt4** ( $\text{C}_{20}\text{H}_{34}\text{N}_6\text{Cl}_4\text{O}_8\text{Pt}_2$ ; FW = 1018.49): C, 23.59%; H, 3.36%; N, 8.25%. Found: C, 23.29%; H, 3.42%; N, 8.36%.  $^1\text{H}$  NMR (200 MHz,  $\text{D}_2\text{O}$ ,  $\delta$ , ppm): 8.16 (m, 2H, C3H, C7H), 9.58 (m, 2H, C4H, C8H), 10.23 (m, 2H, C2H, C6H).  $^{13}\text{C}$  NMR (50 MHz,  $\text{D}_2\text{O}$ ,  $\delta$ , ppm): 130.2 (C3, C7), 142.2 (C4, C8), 147.2 (C4a, C8a), 161.7 (C2, C6). IR (KBr,  $\nu$ ,  $\text{cm}^{-1}$ ):  $\sim$ 3273, 3231 (N–H stretch); 1595, 1513 (C=N/C=N 1,5-naphthyridine group stretch); 1170, 1095, 624 (perchlorate counter ion). UV-vis ( $\text{H}_2\text{O}$ ,  $\lambda_{\text{max}}$ , nm): 317 ( $\epsilon = 10.5 \times 10^3 \text{ M}^{-1} \text{ cm}^{-1}$ ). ESI-HRMS ( $\text{CH}_3\text{CN}$ ):  $[[\{\text{Pt}(\text{dach})\text{Cl}\}_2(\mu\text{-1,5-nphe})]\text{ClO}_4]^+$  ( $m/z = 919.09$ ),  $[\text{Pt}(\text{dach})\text{Cl}(\mu\text{-1,5-nphe})]^+$  ( $m/z = 475.10$ ),  $[\{\text{Pt}(\text{dach})\text{Cl}\}_2(\mu\text{-1,5-nphe})]^{2+}$  ( $m/z = 409.07$ ),  $[\text{Pt}(\text{dach})\text{Cl}]^+$  ( $m/z = 343.05$ ).

Anal. calcd for **Pt5** ( $\text{C}_{14}\text{H}_{26}\text{N}_6\text{Cl}_4\text{O}_8\text{Pt}_2$ ; FW = 938.36): C, 17.92%; H, 2.79%; N, 8.96%. Found: C, 17.81%; H, 2.84%; N, 8.85%.  $^1\text{H}$  NMR (200 MHz,  $\text{D}_2\text{O}$ ,  $\delta$ , ppm): 8.18 (m, 2H, C3H, C7H), 9.58 (d, 2H, C4H, C8H), 10.27 (d, 2H, C2H, C6H).  $^{13}\text{C}$  NMR (50 MHz,  $\text{D}_2\text{O}$ ,  $\delta$ , ppm): 130.4 (C3, C7), 142.3 (C4, C8), 148.0 (C4a, C8a), 161.2 (C2, C6). IR (KBr,  $\nu$ ,  $\text{cm}^{-1}$ ):  $\sim$ 3241, 3135 (N–H stretch); 1599, 1590, 1510 (C=N/C=N 1,5-naphthyridine group stretch); 1096, 1080, 623 (perchlorate counter ion). UV-vis ( $\text{H}_2\text{O}$ ,  $\lambda_{\text{max}}$ , nm): 317 ( $\epsilon = 12.3 \times 10^3 \text{ M}^{-1} \text{ cm}^{-1}$ ). ESI-HRMS ( $\text{CH}_3\text{CN}$ ):  $[[\{\text{Pt}(1,3\text{-pd})\text{Cl}\}_2(\mu\text{-1,5-nphe})]\text{ClO}_4]^+$  ( $m/z = 839.03$ ),  $[\text{Pt}(1,3\text{-pd})\text{Cl}(\mu\text{-1,5-nphe})]^+$  ( $m/z = 435.07$ ),  $[\{\text{Pt}(1,3\text{-pd})\text{Cl}\}_2(\mu\text{-1,5-nphe})]^{2+}$  ( $m/z = 370.04$ ),  $[\text{Pt}(1,3\text{-pd})\text{Cl}]^+$  ( $m/z = 303.02$ ).

Anal. calcd for **Pt6** ( $\text{C}_{18}\text{H}_{34}\text{N}_6\text{Cl}_4\text{O}_8\text{Pt}_2$ ; FW = 995.05): C, 21.74%; H, 3.45%; N, 8.45%. Found: C, 21.54%; H, 3.52%; N, 8.69%.  $^1\text{H}$  NMR (200 MHz,  $\text{D}_2\text{O}$ ,  $\delta$ , ppm): 8.16 (dd, 2H, C3H, C7H), 9.57 (d, 2H, C4H, C8H), 10.27 (d, 2H, C2H, C6H).  $^{13}\text{C}$  NMR (50 MHz,  $\text{D}_2\text{O}$ ,  $\delta$ , ppm): 130.5 (C3, C7), 142.3 (C4, C8), 148.4 (C4a, C8a), 161.0 (C2, C6). IR (KBr,  $\nu$ ,  $\text{cm}^{-1}$ ):  $\sim$ 3255 (N–H stretch); 1603, 1514 (C=N/C=N 1,5-naphthyridine group stretch); 1174, 1089, 625 (perchlorate counter ion). UV-vis ( $\text{H}_2\text{O}$ ,  $\lambda_{\text{max}}$ , nm): 316 ( $\epsilon = 9.0 \times 10^3 \text{ M}^{-1} \text{ cm}^{-1}$ ). ESI-HRMS ( $\text{CH}_3\text{CN}$ ):  $[[\{\text{Pt}(2,2\text{-diMe-1,3-pd})\text{Cl}\}_2(\mu\text{-1,5-nphe})]$

$\text{ClO}_4]^+$  ( $m/z = 895.10$ ),  $[\text{Pt}(2,2\text{-diMe-1,3-pd})\text{Cl}(\mu\text{-1,5-nphe})]^+$  ( $m/z = 463.10$ ),  $[\{\text{Pt}(2,2\text{-diMe-1,3-pd})\text{Cl}\}_2(\mu\text{-1,5-nphe})]^{2+}$  ( $m/z = 397.07$ ),  $[\text{Pt}(2,2\text{-diMe-1,3-pd})\text{Cl}]^+$  ( $m/z = 331.05$ ).

Anal. calcd for **Pt7** ( $\text{C}_{18}\text{H}_{34}\text{N}_6\text{Cl}_4\text{O}_8\text{Pt}_2$ ; FW = 995.05): C, 21.74%; H, 3.45%; N, 8.45%. Found: C, 21.54%; H, 3.52%; N, 8.69%.  $^1\text{H}$  NMR (200 MHz,  $\text{D}_2\text{O}$ ,  $\delta$ , ppm): 8.17 (m, 2H, C3H, C7H), 9.58 (m, 2H, C4H, C8H), 10.23 (m, 2H, C2H, C6H).  $^{13}\text{C}$  NMR (50 MHz,  $\text{D}_2\text{O}$ ,  $\delta$ , ppm): 130.4 (C3, C7), 142.6 (C4, C8), 147.6 (C4a, C8a), 161.1 (C2, C6). IR (KBr,  $\nu$ ,  $\text{cm}^{-1}$ ):  $\sim$ 3233 (N–H stretch); 1595, 1514 (C=N/C=N 1,5-naphthyridine group stretch); 1093, 1080, 623 (perchlorate counter ion). UV-vis ( $\text{H}_2\text{O}$ ,  $\lambda_{\text{max}}$ , nm): 317 ( $\epsilon = 11.0 \times 10^3 \text{ M}^{-1} \text{ cm}^{-1}$ ). ESI-HRMS ( $\text{CH}_3\text{CN}$ ):  $[[\{\text{Pt}(1,3\text{-pnd})\text{Cl}\}_2(\mu\text{-1,5-nphe})]\text{ClO}_4]^+$  ( $m/z = 895.10$ ),  $[\text{Pt}(1,3\text{-pnd})\text{Cl}(\mu\text{-1,5-nphe})]^+$  ( $m/z = 463.10$ ),  $[\{\text{Pt}(1,3\text{-pnd})\text{Cl}\}_2(\mu\text{-1,5-nphe})]^{2+}$  ( $m/z = 397.07$ ),  $[\text{Pt}(1,3\text{-pnd})\text{Cl}]^+$  ( $m/z = 331.05$ ).

### Preparation of drug solutions

Complexes were dissolved in distilled water at a concentration of 10 mM and filtered through a 0.22 mm Millipore filter. These stock solutions were diluted in the culture medium immediately before use. MTT, 3-(4,5-dimethylthiazol-2-yl)-2,5-diphenyl tetrazolium bromide was dissolved ( $5 \text{ mg mL}^{-1}$ ) in a phosphate buffer saline having a pH of 7.20 and filtered through the 0.22 mm Millipore filter before use. All reagents were purchased from Sigma Chemicals.

### Cell culture

CT26, 4T1, LLC1 and MRC-5 cells were purchased from the American Type Culture Collection (ATCC, Manassas, USA). Murine MSC, isolated from the bone marrow of C57BL/6 mice, were purchased from Gibco (catalog no. S1502-100). The cells were maintained in DMEM (Sigma Aldrich, Munich, Germany) supplemented with 10% fetal bovine serum (FBS, Sigma Aldrich, Munich, Germany), penicillin ( $100 \text{ IU mL}^{-1}$ ), and streptomycin ( $100 \mu\text{g mL}^{-1}$ ) under a humidified atmosphere of 95% air/5%  $\text{CO}_2$  at  $37^\circ\text{C}$ . Subconfluent monolayers, in the log growth phase, were harvested by a brief treatment with 0.25% trypsin and 0.02% EDTA in phosphate buffered saline (PBS, Sigma Aldrich, Munich, Germany) and washed three times in serum-free PBS. The number of viable cells was determined by trypan blue exclusion.

### Cytotoxicity assay

The effects of the tested compounds on cell viability were determined using the MTT colorimetric technique.<sup>59</sup> All examined cells were diluted with the growth medium to  $5 \times 10^4$  cells per mL and the aliquots ( $5 \times 10^3$  cells per 100 mL) were placed in individual wells in 96-multiplates. The next day the medium was exchanged with 100  $\mu\text{L}$  of the different compounds, which had been serially diluted 2-fold in the medium to concentrations ranging from 1000  $\mu\text{M}$  to 7.8  $\mu\text{M}$  in the growth medium. Each compound was tested in triplicate. The cells were incubated at  $37^\circ\text{C}$  under a 5%  $\text{CO}_2$  atmosphere for 72 h. After incubation, the supernatant was removed and 15% MTT solution ( $5 \text{ mg mL}^{-1}$  in PBS, 10  $\mu\text{L}$ ) in DMEM medium

without FBS was added to each well. After an additional 4 h of incubation at 37 °C under a 5% CO<sub>2</sub> atmosphere, the medium with MTT was removed and DMSO (150 µL) with glycine buffer (20 µL) was added to dissolve the crystals. The plates were shaken for 10 min. The optical density of each well was determined at 595 nm using a microplate Zenyth 3100 Multimode detector. The percentage of cytotoxicity was calculated using the formula: % cytotoxicity = 100 - ((*E* - *B*)/(*S* - *B*) × 100), where *B* is the background of the medium alone, *S* is the total viability/spontaneous death of untreated target cells, and *E* is the experimental well. Each of the tested complexes was evaluated for cytotoxicity in three separate experiments.

### Apoptosis assay

For the detection of apoptosis, the cells were plated at T25 culture flasks and allowed to grow overnight. After the cells reached subconfluency, the medium was replaced with tested complexes (15 mM). The exposed cells were placed at 37 °C in a 5% CO<sub>2</sub> incubator for 24 h. The cultured cells were washed twice with PBS and resuspended in 1× binding buffer (10× binding buffer: 0.1 M HEPES/NaOH (pH 7.40), 1.4 M NaCl, 25 mM CaCl<sub>2</sub>) at a concentration 1 × 10<sup>6</sup> mL<sup>-1</sup>. Annexin FITC and propidium iodide (PI) were added to 100 mL of the cell suspension and incubated for 15 min at room temperature (25 °C) in the dark. After incubation 400 mL of 1× binding buffer was added to each tube and the stained cells were analyzed within 1 h using FACS Calibur (BD, San Jose, USA) and Flow Jo software (Tri Star). Since, Annexin V FITC staining precedes the loss of membrane integrity that accompanies the later stage identified by PI, Annexin FITC positive, PI negative indicates early apoptosis, while the viable cells are Annexin V FITC negative, PI negative. The cells that are in late apoptosis, or dead are both Annexin V FITC and PI positive.

### Platinum cellular uptake assay

**Sample preparation.** Two × 10<sup>6</sup> LLC1 cells were seeded in a total volume of 5 ml of the RPMI medium, cultured for 24 h, and then exposed to 2 µM of the investigated compounds for 2 h at 37 °C. After exposure, the compound-containing medium was removed, and the cells were washed with 5 ml of PBS and pelleted.

The cells were prepared as follows. The samples were weighed on an analytical balance in a vial (volume of 1.5 ml). Thereafter, 0.3 ml of concentrated nitric acid and 0.1 ml of hydrogen peroxide were added to the sample. The samples were slightly warmed up for about 15 minutes in an aqueous bath at a temperature of 85 °C. Subsequently, the samples were diluted in normal vessels to 10 ml. Thus, the prepared samples were analyzed by ICP-QMS.

**Chemicals and instrumentation.** All used chemicals were of analytical grade (Sigma-Aldrich, Germany). In order to reduce the level of contamination during sample preparation, concentrated nitric acid (65% w/w) was additionally purified by distillation. Hydrogen peroxide was puriss. p.a. 30% (w/w). Platinum, plasma standard solution 1000 µg mL<sup>-1</sup> (Alfa Aesar, Germany) was used for the calibration of the instruments

along with appropriate dilution. Ultra-pure water was used to prepare all standards and samples. Ultra-pure water was prepared by passing double de-ionized water of the Milli-Q system (18.2 MΩ).

The analysis was performed using quadrupole Inductively Coupled Plasma – Mass Spectrometry (ICP-QMS) technique on the instrument Thermo Scientific iCAP Q ICP-MS (Thermo Scientific, UK). Optimized operating conditions of ICP-QMS are summarized in Table S3.† All measurements on ICP-QMS were performed in kinetic energy discrimination (KED) mode with helium as the collision cell gas.

Quantification of all samples was done using external standard calibrations. Six standard solutions of the following platinum concentrations were used 1, 2, 5, 10, 25 and 50 µg L<sup>-1</sup>, along with the blank solution prepared in 1% distilled nitric acid. The correlation coefficient of the regression line was 1.0000.

### Spectroscopic studies on DNA interaction

**Absorption spectroscopic studies.** The interaction of the dinuclear Pt(II) complexes **Pt1–Pt7** with CT-DNA was studied by UV-vis spectroscopy. The platinum(II)-DNA binding experiments were performed in 0.01 M phosphate buffer solution (PBS) at pH 7.40 and 37 °C. The series of the complex-DNA solutions were prepared by mixing of the corresponding dinuclear Pt(II) complex solution (8 µM) with increments of the DNA stock solution (0–16 µM).

**Ethidium bromide displacement studies.** The binding interaction of the **Pt1–Pt7** complexes with DNA was also studied by fluorescence spectroscopy. The fluorescence intensities were measured with an excitation wavelength at 527 nm and fluorescence emission at 612 nm. Ethidium bromide (EtBr) and DNA were mixed in a 1 : 1 molar ratio in 0.01 M PBS at pH 7.40. The possible binding effect of the complexes was investigated step by step after the addition of a certain amount of the complex solution into diluted DNA–EtBr solution at constant concentration. Before the measurements, each system was shaken and incubated at room temperature for 5 min. The emission was recorded in the range 550–750 nm.

### Molecular docking

The key step for the reaction of anticancer chlorido-platinum(II) complexes with the target DNA is the hydrolysis complexes, leading to the activated drug forms.<sup>60</sup> Accordingly, the molecular docking study was performed on hydrolyzed dinuclear Pt(II) complexes. The structures of the aqua derivatives of dinuclear Pt(II) complexes (**W1–W7**, Fig. 4) were optimized by the wb97xd method, with the 6-31g\*\* basis set for non-metal atoms and lanl2dz basis set for Pt. At the same level, the Merz–Kollman atomic charges were calculated for all atoms, according to the scheme *via* the RESP procedure.<sup>61</sup>

The crystal structure of DNA, extracted from the Protein Data Bank (pdb code: 1BNA),<sup>62</sup> was used for the docking study as a target for tested compounds. The selected structure of DNA represents the synthetic double stranded d(CpGpCpGpApApTpTpCpGpCpG) dodecamer with two G≡C

rich regions and one A = T rich region, between them (Fig. 4). The DNA molecule has more than one complete turn of the right-handed B helix, without the DNA intercalation gap. The docking study was also done at the apo form (iron-free form) of the recombinant N-lobe of human serum transferrin (ApoTfN, pdb code 1BP5).<sup>63</sup>

The AutoDock 4.2 software program<sup>64</sup> was used for the preparation of DNA and transportation of protein structures, which includes the addition of hydrogen atoms and removal of water and ligand molecules from the crystal structure. The AutoDockTools program<sup>64</sup> was used to generate the grid and docking parameter files for the optimized structures of tested complexes, and DNA and protein structures. The structure of the biomolecule (DNA or protein) was considered as a rigid species while some bonds of the metal complexes were allowed to rotate freely. A grid box containing the whole biomolecule was used to accommodate the tested compounds during the docking study, while Lamarckian genetic algorithm was used as the search method for virtual screening, with 50 runs for each docking screen. To visualize and analyze the results of docking studies, the *Discovery Studio* (BIOVIA Software product) was used.<sup>65</sup>

## Conflicts of interest

There are no conflicts to declare.

## Acknowledgements

This research has been financially supported by the Ministry of Education, Science and Technological Development of the Republic of Serbia, under Grant No. 172036, 172016, 175069, 172023 and 175103, and the Faculty of Medical Sciences, University of Kragujevac, Serbia (Project No. MP 2014/02). The authors acknowledge the support of the SupraMedChem@Balkans.Net SCOPES Institutional Partnership (Project No. IZ74Z0\_160515) and the Serbian Academy of Sciences and Arts (Project No. F128). Numerical simulations were run on the PARADOX supercomputing facility at the Scientific Computing Laboratory of the Institute of Physics Belgrade, supported in part by the Ministry of Education, Science and Technological Development of the Republic of Serbia. We thank D. Urankar and J. Kljun (University of Ljubljana) for HRMS measurements.

## Notes and references

- C. Johnstone, K. Suntharalingam and S. J. Lippard, *Chem. Rev.*, 2016, **116**, 3436–3486.
- N. J. Wheate, S. Walker, G. E. Craig and R. Oun, *Dalton Trans.*, 2010, **39**, 8113–8127.
- L. Kelland, *Nat. Rev. Cancer*, 2007, **7**, 573–584.
- E. R. Jamieson and S. J. Lippard, *Chem. Rev.*, 1999, **99**, 2467–2498.
- J. Reedijk, *Chem. Rev.*, 1999, **99**, 2499–2510.
- N. Farrell, *Comments Inorg. Chem.*, 1995, **16**, 373–389.
- J. Reedijk, *Proc. Natl. Acad. Sci. U. S. A.*, 2003, **100**, 3611–3616.
- N. Farrell and S. Spinelli, Dinuclear and Trinuclear Platinum Anticancer Agents, in *Uses of Inorganic Chemistry in Medicine*, ed. N. Farrell, Royal Society of Chemistry, London, 1999, pp. 124–134.
- S. Komeda, M. Lutz, A. L. Spek, M. Chikuma and J. Reedijk, *Inorg. Chem.*, 2000, **39**, 4230–4236.
- S. Komeda, M. Lutz, A. L. Spek, Y. Yamanaka, T. Sato, M. Chikuma and J. Reedijk, *J. Am. Chem. Soc.*, 2002, **124**, 4738–4746.
- C. Manzotti, G. Pratesi, E. Menta, R. Di Domenico, E. Cavalletti, H. H. Fiebig, L. R. Kelland, N. Farrell, D. Polizzi, R. Supino, G. Pezzoni and F. Zunino, *Clin. Cancer Res.*, 2000, **6**, 2626–2634.
- X. Han and X. Gao, *Curr. Med. Chem.*, 2001, **8**, 551–581.
- S. Neidle and C. M. Nunn, *Nat. Prod. Rep.*, 1998, **15**, 1–15.
- G. Bischoff and S. Hoffmann, *Curr. Med. Chem.*, 2002, **9**, 312–348.
- J. N. Lisgarten, M. Coll, J. Portugal, C. W. Wright and J. Aymami, *Nat. Struct. Biol.*, 2002, **9**, 57–60.
- D. E. Wemmer, *Annu. Rev. Biophys. Biomol. Struct.*, 2000, **29**, 439–461.
- J. Ren and J. B. Chaires, *Biochemistry*, 1999, **38**, 16067–16075.
- S. I. Komeda, Y. Qu, J. B. Mangrum, A. Hegmans, L. D. Williams and N. P. Farrell, *Inorg. Chim. Acta*, 2016, **452**, 25–33.
- D. P. Ašanin, M. D. Živković, S. Rajković, B. Warzajtis, U. Rychlewska and M. I. Djuran, *Polyhedron*, 2013, **51**, 255–262.
- S. Rajković, D. P. Ašanin, M. D. Živković and M. I. Djuran, *Polyhedron*, 2013, **65**, 42–47.
- S. Rajković, M. D. Živković, B. Warzajtis, U. Rychlewska and M. I. Djuran, *Polyhedron*, 2016, **117**, 367–376.
- S. Rajković, U. Rychlewska, B. Warzajtis, D. P. Ašanin, M. D. Živković and M. I. Djuran, *Polyhedron*, 2014, **67**, 279–285.
- L. Senerović, M. D. Živković, A. Veselinović, A. Pavić, M. I. Djuran, S. Rajković and J. Nikodinović-Runić, *J. Med. Chem.*, 2015, **58**, 1442–1451.
- B. Đ. Glišić, B. Warzajtis, N. S. Radulović, U. Rychlewska and M. I. Djuran, *Polyhedron*, 2015, **87**, 208–214.
- B. Warzajtis, B. Đ. Glišić, N. S. Radulović, U. Rychlewska and M. I. Djuran, *Polyhedron*, 2014, **79**, 221–228.
- S. Chattopadhyay, P. Chakraborty, M. G. B. Drew and A. Ghosh, *Inorg. Chim. Acta*, 2009, **362**, 502–508.
- K. N. Lazarou, I. Chadjistamatis, A. Terzis, S. P. Perlepes and C. P. Raptopoulou, *Polyhedron*, 2010, **29**, 1870–1879.
- T. C. Johnstone, K. Suntharalingam and S. J. Lippard, *Chem. Rev.*, 2016, **116**, 3436–3486.
- A. Ehnbohm, S. K. Ghosh, K. G. Lewis and J. A. Gladysz, *Chem. Soc. Rev.*, 2016, **45**, 6799–6811.
- G. R. Stockwell and J. M. Thornton, *J. Mol. Biol.*, 2006, **356**, 928–944.

- 31 R. M. Knechtel, J. Antoon, C. Rullmann, R. Boelens and R. Kaptein, *J. Mol. Biol.*, 1994, **235**, 318–324.
- 32 K. Bastard, A. Thureau, R. Lavery and C. Prevost, *J. Comput. Chem.*, 2003, **24**, 1910–1920.
- 33 A. A. Adesokan, V. A. Roberts, K. W. Lee, R. D. Lins and J. M. Briggs, *J. Med. Chem.*, 2004, **47**, 821–828.
- 34 V. A. Roberts, D. A. Case and V. Tsui, *Proteins*, 2004, **57**, 172–187.
- 35 J. B. Mangrum and N. P. Farrell, *Chem. Commun.*, 2010, **46**, 6640–6650.
- 36 S. Komeda, T. Moulaei, K. K. Woods, M. Chikuma, N. P. Farrell and L. D. Williams, *J. Am. Chem. Soc.*, 2006, **128**, 16092–16103.
- 37 H. Rauter, R. Di Domenico, E. Menta, A. Oliva, Y. Qu and N. Farrell, *Inorg. Chem.*, 1997, **36**, 3919–3927.
- 38 N. Farrell, Y. Qu, U. Bierbach, M. Valsecchi and E. Menta, in *30 years of Cisplatin – Chemistry and Biochemistry of a Leading Anticancer Drug*, ed. B. Lippert, Verlag, 1999, pp. 479–496.
- 39 T. D. McGregor, J. Kasparkova, K. Nepelchova, O. Novakova, H. Penazova, O. Vrana, V. Brabec and N. Farrell, *J. Biol. Inorg. Chem.*, 2002, **7**, 397–404.
- 40 P. Wu, M. Kharatishvili, Y. Qu and N. Farrell, *J. Inorg. Biochem.*, 1996, **63**, 9–18.
- 41 T. D. McGregor, W. Bousfield, Y. Qu and N. Farrell, *J. Inorg. Biochem.*, 2002, **91**, 212–219.
- 42 A. Prisecaru, Z. Molphy, R. G. Kipping, E. J. Peterson, Y. Qu, A. Kellett and N. P. Farrell, *Nucleic Acids Res.*, 2014, **42**, 13474–13487.
- 43 A. Harris, Y. Qu and N. P. Farrell, *Inorg. Chem.*, 2005, **44**, 1196–1198.
- 44 J. Malina, N. P. Farrell and V. Brabec, *Inorg. Chem.*, 2014, **53**, 1662–1671.
- 45 J. Malina, N. P. Farrell and V. Brabec, *Angew. Chem.*, 2014, **53**, 12812–12816.
- 46 A. Prisecaru, Z. Molphy, R. G. Kipping, E. J. Peterson, A. Kellett and N. P. Farrell, *Nucleic Acids Res.*, 2014, **42**, 13474–13487.
- 47 A. L. Harris, X. Yang, A. Hegmans, L. Povirk, J. J. Ryan, L. Kelland and N. P. Farrell, *Inorg. Chem.*, 2005, **44**, 9598–9600.
- 48 B. T. Benedetti, E. J. Peterson, P. Kabolizadeh, A. Martínez, R. G. Kipping and N. P. Farrell, *Mol. Pharmaceutics*, 2011, **8**, 940–948.
- 49 E. I. Montero, B. T. Benedetti, J. B. Mangrum, M. J. Oehlsen, Y. Qu and N. P. Farrell, *Dalton Trans.*, 2007, 4938–4942.
- 50 V. Brabec, O. Hrabina and J. Kasparkova, *Coord. Chem. Rev.*, 2017, **351**, 2–31.
- 51 F. Dimiza, S. Fountoulaki, A. N. Papadopoulos, C. A. Kontogiorgis, V. Tangoulis, C. P. Raptopoulou, V. Psycharis, A. Terzis, D. P. Kessissoglou and G. Psomas, *Dalton Trans.*, 2011, **40**, 8555–8568.
- 52 F. Dimiza, F. Perdih, V. Tangoulis, I. Turel, D. P. Kessissoglou and G. Psomas, *J. Inorg. Biochem.*, 2011, **105**, 476–489.
- 53 S. Komeda, G. V. Kalayda, M. Lutz, A. L. Spek, Y. Yamanaka, T. Sato, M. Chikuma and J. Reedijk, *J. Med. Chem.*, 2003, **46**, 1210–1219.
- 54 S. C. Dhara, *Indian J. Chem.*, 1970, **8**, 193–194.
- 55 S. U. Milinković, T. N. Parac, M. I. Djuran and N. M. Kostić, *J. Chem. Soc., Dalton Trans.*, 1997, 2771–2776.
- 56 H. Hohmann and R. van Eldik, *Inorg. Chim. Acta*, 1990, **174**, 87–92.
- 57 M. D. Živković, D. P. Ašanin, S. Rajković and M. I. Djuran, *Polyhedron*, 2011, **30**, 947–952.
- 58 G. Mahal and R. van Eldik, *Inorg. Chem.*, 1985, **24**, 4165–4170.
- 59 T. Mosmann, *J. Immunol. Methods*, 1983, **16**, 55–63.
- 60 C. Zhu, J. Raber and L. A. Eriksson, *J. Phys. Chem. B*, 2005, **109**, 12195–12205.
- 61 C. I. Bayly, P. Cieplak, W. D. Cornell and P. A. Kollman, *J. Phys. Chem.*, 1993, **97**, 10269–10280.
- 62 H. R. Drew, R. M. Wing, T. Takano, C. Broka, S. Tanaka, K. Itakura and R. E. Dickerson, *Proc. Natl. Acad. Sci. U. S. A.*, 1981, **78**, 2179–2183.
- 63 L. Wang and H. Yan, *Biochemistry*, 1998, **37**, 13021–13032.
- 64 G. M. Morris, R. Huey, W. Lindstrom, M. F. Sanner, R. K. Belew, D. S. Goodsell and A. J. Olson, *J. Comput. Chem.*, 2009, **30**, 2785–2791.
- 65 Dassault Systèmes BIOVIA, *Discovery Studio Modeling Environment, Release 2017*, 2016.